

MIT Open Access Articles

Engineered yeast for enhanced CO2 mineralization

The MIT Faculty has made this article openly available. **Please share** how this access benefits you. Your story matters.

Citation: Barbero, Roberto, Lino Carnelli, Anna Simon, Albert Kao, Alessandra d'Arminio Monforte, Moreno Riccò, Daniele Bianchi, and Angela Belcher. "Engineered Yeast for Enhanced CO2 Mineralization." *Energy & Environmental Science* 6, no. 2 (2013): 660.

As Published: <http://dx.doi.org/10.1039/c2ee24060b>

Publisher: Royal Society of Chemistry

Persistent URL: <http://hdl.handle.net/1721.1/91613>

Version: Author's final manuscript: final author's manuscript post peer review, without publisher's formatting or copy editing

Terms of use: Creative Commons Attribution-Noncommercial-Share Alike





Published in final edited form as:

Energy Environ Sci. 2013 February 1; 6(2): 660–674. doi:10.1039/C2EE24060B.

Engineered yeast for enhanced CO₂ mineralization†

Roberto Barbero^a, Lino Carnelli^b, Anna Simon^c, Albert Kao^d, Alessandra d'Arminio Monforte^e, Moreno Riccò^f, Daniele Bianchi^g, and Angela Belcher^h

Roberto Barbero: barbero@mit.edu; Lino Carnelli: lino.carnelli@eni.com; Anna Simon: anna.simon@lifesci.ucsb.edu; Albert Kao: akao90@gmail.com; Alessandra d'Arminio Monforte: alessandra.d.arminio.monforte@eni.com; Moreno Riccò: moreno.riccò@eni.com; Daniele Bianchi: daniele.bianchi2@eni.com; Angela Belcher: belcher@mit.edu

^aDepartment of Biological Engineering, The David H. Koch Institute for Integrative Cancer Research, Massachusetts Institute of Technology, 32 Vassar Street, Building 76-561, Cambridge, MA 02142, USA. Tel: +1 617 324 3400

^bEni s.p.a – Research Center for Non-Conventional Energy, Istituto Eni Donegani, Via Fauser, 4 – 28100 Novara (NO), Italy. Fax: +39 032 144 7506; Tel: +39 032 144 7614

^cUC Santa Barbara, Santa Barbara, CA, USA. Fax: +1 805 893 4120; Tel: +1 805 893 5845

^dMassachusetts Institute of Technology, 400 Memorial Drive, Cambridge, MA, USA. Tel: +1 603 770 8225

^eEni s.p.a – Research Center for Non-Conventional Energy, Istituto Eni Donegani, Via Fauser, 4 – 28100 Novara (NO), Italy. Fax: +39 032 144 7506; Tel: +39 032 144 7476

^fEni s.p.a – Research Center for Non-Conventional Energy, Istituto Eni Donegani, Via Fauser, 4 – 28100 Novara (NO), Italy. Fax: +39 032 144 7506; Tel: +39 032 144 7484

^gEni s.p.a – Research and Technology Innovation, Via Fauser, 4 – 28100 Novara (NO), Italy. Tel: +39 0321 447655

^hDepartment of Materials Science and Engineering and Department of Biological Engineering, The David H. Koch Institute for Integrative Cancer Research, Massachusetts Institute of Technology, 32 Vassar Street, Building 76-561, Cambridge, MA 02142, USA. Fax: +1 617 324 3300; Tel: +1 617 324 2800

Abstract

In this work, a biologically catalyzed CO₂ mineralization process for the capture of CO₂ from point sources was designed, constructed at a laboratory scale, and, using standard chemical process scale-up protocols, was modeled and evaluated at an industrial scale. A yeast display system in *Saccharomyces cerevisiae* was used to screen several carbonic anhydrase isoforms and mineralization peptides for their impact on CO₂ hydration, CaCO₃ mineralization, and particle settling rate. Enhanced rates for each of these steps in the CaCO₃ mineralization process were confirmed using quantitative techniques in lab-scale measurements. The effect of these enhanced

†Electronic supplementary information (ESI) available. See DOI: 10.1039/c2ee24060b

Contributions

R.B. and A.B. conceived the idea and designed the experiments. R.B., L.C. A.S., A.K., A.M., and M.R. performed the experiments and analyzed the data. R.B., L.C., A.S. and A.B. co-wrote the paper and all authors discussed the results and commented on the manuscript.

rates on the CO₂ capture cost in an industrial scale CO₂ mineralization process using coal fly ash as the CaO source was evaluated. The model predicts a process using bCA2- yeast and fly ash is ~10% more cost effective per ton of CO₂ captured than a process with no biological molecules, a savings not realized by wild-type yeast and high-temperature stable recombinant CA2 alone or in combination. The levelized cost of electricity for a power plant using this process was calculated and scenarios in which this process compares favorably to CO₂ capture by MEA absorption process are presented.

1 Introduction

Atmospheric CO₂ levels have increased over the last 150 years, contributing significantly to global climate change. Several strategies for reducing CO₂ emission rates have been proposed, and substantially decreasing emissions will likely require a combination of altering the manner and amount of energy consumption, reducing the release of greenhouse gases during energy production and adaptation to a changing planet. One strategy that will be an important component of the human response to global climate change is carbon capture and storage (CCS).

Mineralization of CO₂ is an attractive CCS technology for two reasons. First, mineralization is a relatively permanent sequestration method. Carbonate minerals are stable on the order of thousands of years, and thus are unlikely to result in CO₂ release back into the atmosphere.¹ Furthermore, the mechanical strength and stability of mineral carbonates makes them well-suited as inputs for building materials or manufacturing processes; potential buyers of the material might help offset the cost of CO₂ capture. However, there are several challenges involved in applying mineralization of CO₂ as a commercial CCS technology. Carbonate mineralization requires stoichiometric amounts of divalent cations and alkalinity, and the physical and economic availability and accessibility of these sources must be addressed.²⁻⁴ Also, the established mineralization process either occurs slowly or requires extreme and costly operating conditions, which contributes to a higher CO₂ capture cost and use of natural resources.

There are many examples of biologically catalyzed CO₂ mineralization, including in mollusk shells, sea urchin spicules, coral, and avian eggshells.⁵⁻⁹ All of these processes occur under benign conditions, and we hypothesized that we could use a biomimetic process to reduce the CO₂ capture cost of carbonate mineralization. To this end, we designed, built, modeled the scale-up of, and evaluated a biologically catalyzed system that can be used to capture CO₂ directly from the flue gas of a fossil fuel power plant.

2 Results

Our aim for this work is to put forward a novel CCS system that utilizes a well-known, safe and industrially scalable organism and to offer estimates of the cost at a process scale. We demonstrate that *S. cerevisiae*, with which the food services industry has decades of experience at a process scale, can be engineered to enhance the mineralization rate of CO₂. Moreover, our process model, which we developed based on our own bench scale measurements combined with data from the literature and which is grounded in the

fundamentals of the chemical process design field, predicts that a process utilizing this organism would cost less than either a process without biomolecules or one that utilized recombinant carbonic anhydrase.

Several groups have investigated biocatalytic approaches to CO₂ sequestration, proposing the use of carbonic anhydrase engineered to be stable at higher temperatures, carbonic anhydrase anchored to the surface of the bacteria *Escherichia coli* to enhance CO₂ dissolution or the use of bacteria and cyanobacteria for enhanced mineralization of CO₂.^{10–18} To enable ready commercialization and industrial scale up, we engineered the well-known, safe, and industrially scalable organism, *S. cerevisiae*, to enhance the rates of CO₂ hydration, CaCO₃ mineralization, and the settling rate of the mineralized CaCO₃. This approach provided more control over the molecular components in the system and their relative contributions to the mineralization process, which, in turn, enabled the design and evaluation of an industrial scale process.

2.1 Enhanced CO₂ hydration

To accelerate the hydration rate of aqueous CO₂, we expressed the enzyme carbonic anhydrase on the surface of the yeast cells using yeast display.^{19,20} We tested three isoforms of carbonic anhydrase, human carbonic anhydrase II (hCA2), bovine carbonic anhydrase II (bCA2) and a carbonic anhydrase isoform from the mildly thermophilic organism *Streptococcus thermophilus* (CAH). As demonstrated in Fig. 1, all three isoforms were expressed in active form on the surface of the *S. cerevisiae* cells. When displayed on the surface of the yeast, both the bCA2 (bCA2-yeast) and CAH isoforms (CAH-yeast) had activities comparable to or better than that of a commercially purchased soluble bCA2 (purified from cow erythrocytes), whereas the hCA2 appeared to have lower activity. The bCA2 and CAH displayed on yeast were quite stable over a range of temperature and pH, as shown in ESI Fig. 1.[†] The samples were stored at 50 °C for up to 7 days and were also exposed to pH conditions ranging from low to neutral for 16 hours at 4 °C. In all cases, the bCA2-yeast performed as well as the soluble bCA2. Notably, the bCA2-yeast retained roughly 20% of its activity after 3 days at 50 °C. These results demonstrated that bCA2 displayed on the surface of yeast cells has comparable activity and stability to soluble bCA2, which has a reported turnover rate of $1 \times 10^6 \text{ s}^{-1}$.²¹ In order to account for unforeseen process effects that might decrease the efficiency of bCA2-yeast, a conservative turnover rate of $6 \times 10^5 \text{ s}^{-1}$ was chosen for the value to be used in the scaled-up process design (see Table 2).

2.2 Enhanced carbonate mineralization

To catalyze the formation of carbonate mineral from bicarbonate we next identified a set of optimal mineralization peptides and displayed them on the surface of *S. cerevisiae* cells (see Table 1). To determine which peptides were most effective under reactor conditions we screened for enhanced mineralization of calcium carbonate. Two of the peptides, GPA and N66, came from naturally occurring proteins that interact with calcium or CaCO₃. Three control peptides with no negative amino acids or with positive amino acid repeats were

[†]Electronic supplementary information (ESI) available. See DOI: 10.1039/c2ee24060b

chosen: LPC, KQY, and FLK. Two synthetic peptides that previously were shown to promote the growth of CaCO_3 in solution were chosen: $(\text{D}_3\text{G})_6\text{D}_3$ and $(\text{D}_3\text{S})_6\text{D}_3$.²² Finally, shortened versions of those two latter peptides were chosen, in order to test the sensitivity of the mineralization rate to the length of the peptide displayed.

The expression of these peptides was verified and quantified using FACS, described in the ESI section.[†] All of the peptides were displayed at high levels on the surfaces of the *S. cerevisiae*. The mineralization activity of each peptide-yeast strain and a no peptide strain of *S. cerevisiae* were assayed at concentrations of 2×10^7 cells per mL and 2×10^8 cells per mL (1 OD_{600} and 10 OD_{600} , respectively), along with a no yeast control sample. The total number of peptides per 2×10^7 cells is shown in Table 1 and the results of the CaCO_3 mineralization assay are shown in Fig. 2. At 2×10^7 cells per mL there is little effect on the mineralization rate, when compared to the no yeast sample. At 2×10^8 cells per mL, however, several of the yeast-displayed peptides increased the mineralization rate 50% or more. The cells that are not displaying any peptide also increased the mineralization rate of CaCO_3 in a dose-dependent manner. This is not surprising, given that *S. cerevisiae* cells are covered in negatively charged biomolecules and it has been previously reported that CaCO_3 can be mineralized on the surface of *S. cerevisiae* cells.²³

The formation of CaCO_3 on the surface of the cells was verified by analyzing the cells with light microscopy, polarized light microscopy and by XRD. Representative microscope images from an N66-yeast sample with mineralized carbonate are shown in ESI Fig. 2a and b.[†] These images demonstrated that the crystals are bound to the surfaces of cells and that they change the polarization of the light. XRD analyses of the same N66-yeast mineralization sample, shown in ESI Fig. 2c,[†] confirm that calcite is the only crystal present in the sample.

2.3 From CO_2 to CaCO_3

A lab-scale CO_2 mineralization reactor, described in the Experimental section and shown in ESI Fig. 4,[†] was used to confirm that bCA2-yeast could enhance the conversion of gaseous CO_2 (from a mock flue gas of 15% CO_2 and 85% N_2) to mineralized carbonate at room temperature. The performance of the bCA2- yeast was compared to that of soluble bCA2 (at the same concentration of enzyme) and to a sample with no biomolecules (see ESI Table 1[†]).

2.4 Selection of cation and alkalinity source

The aqueous mineralization of CO_2 requires two material inputs, a divalent cation such as calcium or magnesium and a source of alkalinity such as hydroxide ions. While cations are readily available, alkalinity is harder to obtain on an industrial scale. There are several possible sources of alkalinity, including reactive mineral deposits, industrial byproducts (such as coal fly ash or paper mill ash), electrochemically generated alkalinity from brines or seawater, or non-reactive mineral deposits, discussed in detail elsewhere.²⁻⁴

While the electrochemical production of alkalinity allows for the capture of CO_2 on a global scale, this approach adds additional energy demand to the CO_2 capture process, thus

increasing the cost of the process. To reduce process cost, this work proposes to use a smaller scale but less expensive source of alkalinity—alkaline industrial byproducts such as fly ash or paper mill ash.

Fly ash produced from a single 200 megawatt coal fired power plant is approximately 40 kton per year. Assuming a calcium oxide content of 17% by weight, this amount of fly ash could sequester about 6.5 kton per year of CO₂, or roughly 0.5% of the CO₂ generated by the power plant. Thus, in order to identify the cost feasibility of the simplest process, fly ash from the power plant is used as the source for both the divalent cations and the alkalinity.

2.5 Development of an industrial-scale process for biologically catalyzed CO₂ mineralization

The bench scale experiments were conducted to demonstrate the biochemical feasibility of the process and to measure the kinetics of the various stages of the reaction. Using the kinetic measurements from these experiments, we were able to identify the best types and dimensions of process equipment that could be used at an industrial scale. The types of equipment chosen for the industrial scale process are those that are normally used for these types of reactions.^{24–26} The mineralization rates and the CO₂ hydration rate parameters that were used for the dimensioning of the process components were taken from the lab-scale measurements and are summarized in Table 2.

We recognized the limitations of using a bubble reactor in an industrial-scale operation (low mass transfer from the gaseous to the liquid phase as well as difficulty in ensuring complete mixing at a large scale), so we chose to use a spray column for the absorption of CO₂ in the industrial scale process. A spray-based column can operate with a small pressure drop in air and allows for a large gas to liquid surface area interface.²⁷ The use of spray columns for CO₂ capture has been addressed by others, at both a laboratory scale (height of 0.3 m) and a scale that is similar to the spray column that we use in our industrial scale model (heights of 3.8 m vs. 10 m), and previous work shows that CO₂ capture would benefit from CO₂ hydration rate enhancement.^{27,28}

To compare the effects of various process parameters, a base case using bCA2-yeast and fly ash was designed (see Fig. 3, Table 3 and Table 4). The following assumptions were made in order to develop the base-case process model:

1. CO₂ flux = 6.7 ktons per year × 95% capacity factor = 5.09 moles CO₂ per second. Capacity factors for CO₂ capture plants are expected to be higher than the capacity factor for the corresponding power plant. The range of capacity factors for power plants is 75–95%. Thus we selected a capacity factor on the high end of that range.^{29,30}
2. Flue gas rate = 3000 N m³ h⁻¹.
3. The flue gas has a composition, in percent volume, of N₂ = 73.8, O₂ = 3.4, CO₂ = 13.7, H₂O = 9.1 and is released from the flue stack at a temperature of 85 °C and atmospheric pressure.

4. The reaction kinetics measured using the mock flue gas are representative of the kinetics for real flue gas which contains acidifying HCl and other components that could affect pH and ionic strength in the CO₂ capture reactor. Any differences in the kinetics for the two types of flue gas would affect both the no yeast and the yeast-based systems discussed below.
5. A heat exchanger cools the flue gas to 40 °C to reach the optimal temperature for enzyme stability and a fan blows it into the absorber.
6. The efficiency in CO₂ absorption by the CaO has been set at 85% on the basis of the results reported in the literature (which ranged from 80% to 98%)²⁴⁻²⁶ All of the reacted CaO forms CaCO₃.
7. The fly ash has a composition, in weight percent, of SiO₂ = 50, Al₂O₃ = 25, Fe₂O₃ = 8, CaO = 17, which corresponds to class C fly ash.
8. The rate of fly ash addition to the process is roughly 5 ton per hour.
9. A single strain of yeast is used (bCA2-yeast), with a CO₂ hydration rate parameter of $6 \times 10^5 \text{ s}^{-1}$, a CaCO₃ mineralization rate of $6.3 \times 10^{-4} \text{ moles CaCO}_3 \text{ L}^{-1} \text{ s}$ and at a concentration of 1.1×10^8 cells per mL in the reactors.
10. Water is added to the system at a rate of 2.5 tons h⁻¹ with a circulating rate of roughly 70 tons h⁻¹ such that the slurry in the absorption column is maintained at a concentration of 7.5% (by weight) solids. Water is added to compensate for evaporation in the absorption column and for the liquid that exits the process with the solids.
11. After mineralization, there are two solid separation stages: the first is a gravity settling stage that leads to a solid content of 25% (from 8%) and the second is a press filtration stage (with two filter presses working in alternate operation) that leads to a solid content of 85%. Finally, a dryer is used to increase the solids content up to 95.5%.
12. The bCA2-yeast is not separated from the solids (because the carbonate mineralizes on them), but the water from the settling and filter press stages can be recirculated. The water from the settling stage is cooled to 35°C before being recirculated to prevent overheating of the bCA2-yeast.
13. The spray column absorber allows for a gas flow rate of roughly 2 m s⁻¹ with a pressure drop of just a few millibars. The diameter of the spray column (1.2 m) is determined by the speed of the gas flow inside, which is set to a standard rate of 0.75 m s⁻¹. With a liquid hold-up of 5%, a slurry concentration of 7.5%, and a concentration of 1.1×10^8 cells per L, a 10 m column can absorb the CO₂ at the assumed CO₂ flux.
14. The mineralized CO₂ product can be sold to a downstream user, which allows the process to claim a landfill non-use tipping fee credit of \$17.89 tonne⁻¹.³¹

2.6 Impact of bCA2-yeast on industrial-scale process

In the laboratory measurements, the bCA2-yeast was shown to enhance the rates of CO₂ hydration, CaCO₃ mineralization, and particle settling (see ESI[†] for calculations). Without bCA2-yeast in the industrial-scale process, the absorber S3, the mineralization reactor S4, and the settling reactor M2 would all have to be scaled up to handle the slower reaction rates. Using the catalyzed and uncatalyzed reaction rates measured in the lab (Table 2), the sizes and costs for each of the larger reactors was calculated and they are reported in ESI Table 4.[†] The ESI[†] section contains detailed calculations for each of the large scale reactors.

2.7 Alternative sources of CA2

There are alternate ways to procure a suitable quantity of carbonic anhydrase to catalyze the CO₂ hydration in this process and it is useful to compare the costs of those approaches to the cost of the approach proposed in this work. The amount of carbonic anhydrase that is required can be calculated using the following equation:

$$\text{CA2 flux} = (\text{Volumetric rate}_{\text{absorber}}) \times \left(\frac{\text{cells}}{\text{L}}\right) \left(\frac{\text{CA2}}{\text{cell}}\right) \left(\frac{\text{mole}}{\text{CA2}}\right) \left(\frac{\text{grams CA2}}{\text{mole}}\right) \approx 38 \text{ g h}^{-1}$$

where the volumetric rate in the absorber is $6.98 \times 10^4 \text{ L h}^{-1}$, the concentration of cells in the absorber $1.1 \times 10^8 \text{ cells per mL}$, the number of enzymes per cell is 100,000 (measured using methods described in Experimental section), and the molecular weight of CA2 = 30 kDa.

The bCA2 that was used during the development of this process was purified from bovine red blood cells and is available for purchase at a cost of $\$1.25 \text{ mg}^{-1}$. Assuming that economies of scale could lower this cost by 100 (and ignoring the number of cows that would need to be regularly bled to provide 38 grams of enzyme per hour), this would still result in over \$4 million per year.

Recently, the use of high-temperature stable CA2 has been suggested for CO₂ capture.^{17,18} The impact that a recombinantly produced CA2 isoform, stable for 2 hours at 60 °C, would have on the CO₂ mineralization process was evaluated and compared to the bCA2-yeast process. To our knowledge, no one has reported on the cost of recombinantly produced CA2 at an industrial scale. There are, however, several estimates of the cost of production of a wide variety of industrial enzymes, including those with applications in biofuels, detergents, food, and agriculture. These production costs range between $\$10 \text{ kg}^{-1}$ and $\$40 \text{ kg}^{-1}$.^{32–34} To assuage any concern about bias toward the bCA2-yeast process, it was assumed that high-temperature stable CA2 could be purchased at a cost at the lowest end of this range, $\$10 \text{ kg}^{-1}$, for use in our process. The impact of the cost of purchased CA2 was calculated by recalculating the operating cost of the process by replacing the yeast, copper sulphate, and glucose with recombinant CA2 (0.038 kg h^{-1}) in the operating cost section of the economic evaluation table (Table 5).

2.8 Heavy metal content in mineralized CO₂ product using coal fly ash and paper mill ash as CaO source

To evaluate the utility of coal fly ash and paper mill ash as CaO sources, we mineralized CO₂ using both and analyzed the product for heavy metal content. Both CaO sources produced material that met the Toxics in Packaging Materials requirement of less than 100 ppm of all five of these metals in total, which means that this product could safely be used as precursors for downstream products such as building materials. See ESI Table 11[†] for the results of this analysis.

2.9 Evaluation of process modifications

Using the bCA2-yeast and fly ash process presented in Fig. 3 as the base case (process 1 in Table 5), the methodology described in the Experimental section below was used to calculate the cost of CO₂ capture for the process. Using the same methodology, eight modifications to the process were compared, including alternate biological catalysts and CaO sources. Descriptions and costs of CO₂ capture for each are reported in Table 5.

Briefly, the modifications that were investigated can be grouped into three categories: (1) modifications that would be expected to decrease CO₂ capture cost by reducing capital equipment expenditures; (2) modifications that investigate the benefit of bCA2-yeast compared to other (or no) biological components; and (3) modifications that investigate the use of other CaO sources.

Since capital equipment expenses are the major driver of process cost, the most expensive piece of equipment (the plate dryer, E3) was removed from the process model (process 3 in Table 5). The removal of this piece of equipment results in lower equipment costs, but also in an end product that has 15% water. If the end-user can tolerate a wetted product, then this would be a reasonable change to make to the process in order to reduce the CO₂ capture costs. However, if the end-user will not accept wetted product, the removal of the drier leads to a higher CO₂ capture cost because the product has to be disposed of in the landfill (see ESI Table 9[†]).

A hypothetical 10 enhancement in the mineralization rate (process 2 in Table 5) would mean that the reaction was fast enough that the mineralization reactor could be removed and the mineralization would be completed in the absorber and downstream pipes. Our model predicted that this would only lead to a \$4% decrease in the CO₂ capture cost compared to the base case, which does suggest a possible area for future exploration.

To demonstrate the benefit of the bCA2-yeast strain to a CO₂ mineralization process, we compared the cost of CO₂ capture to a process without biological molecules (process 4), to a process with a high-temperature stable recombinant CA2 isoform that would enhance CO₂ hydration and that would require less cooling of flue gas (process 6), to a wild-type yeast strain that would enhance CaCO₃ mineralization and settling rates (process 5), and to a two component system with high-temperature stable CA2 and wild-type yeast that would enhance CO₂ hydration, CaCO₃ mineralization, and the settling rate and that would require less cooling of the flue gas. The model predicts that the process using bCA2-yeast and fly ash is \$10% more cost effective per ton of CO₂ captured than a process with no biological

molecules, a savings not realized by the wild-type yeast or high-temperature stable recombinant CA2 alone or in combination (Table 5).

Finally, two alternate sources of CaO were evaluated in combination with bCA2-yeast: paper mill ash from a plant that uses the Kraft process (process 8 in Table 5) and CaO that has been leached from fly ash prior to the addition of the flue gas CO₂ (process 9 in Table 5). These two processes would result in higher concentrations of CaCO₃ in the final product (which might be appealing to a downstream user). While both of these processes have smaller capital equipment costs, the preleaching of the CaO process does not divert as much fly ash from the landfill, and thus it is more expensive per ton of CO₂ captured. However, if landfill tipping fee credits are ignored for all processes, then both of the alternate CaO sources lead to lower cost CO₂ capture (ESI Table 9[†]) when compared to the base case.

2.10 Levelized cost of electricity for bCA2-yeast and fly ash mineralization process

To provide a useful benchmark for the cost of the biologically catalyzed CO₂ capture process proposed in this work, the levelized cost of electricity (LCOE) was calculated for a pulverized coal subcritical power plant using this process for post combustion CO₂ capture. Since landfill tipping fee credits and the post-process sale of the mineralized CO₂ both contribute to the final cost of the process, and, since both are variable, we felt it was most informative to investigate ranges of values.

Others have reported landfill tipping fees for fly ash of \$17.89 tonne⁻¹ and \$39 tonne⁻¹, which is consistent with, if not a bit lower than, recent national landfill tipping fee surveys.^{12,31,35} Thus, we chose a range of \$0 tonne⁻¹ to \$40 tonne⁻¹ for the landfill tipping fee credit.

We assumed that a likely buyer for our mineralized CO₂ might be an entity in the building materials industry, since there are several building materials already on the market that incorporate fly ash, including bricks and concrete, and there are many examples of CaCO₃ incorporation into building materials. Fly ash prices have been reported to range from \$17 tonne⁻¹ to \$40 tonne⁻¹ and 2006 CaCO₃ prices ranged from \$66 tonne⁻¹ to \$309 tonne⁻¹.^{36,37} Thus, a range of \$0 tonne⁻¹ to \$40 tonne⁻¹ for product sale price seemed reasonable. The results of this analysis for the bCA2-yeast and fly ash process are shown in Fig. 4 and for a process with no biological components in ESI Fig. 6.[†] We benchmarked our process against a widely accepted baseline case utilizing monoethanolamine (MEA) absorption for post combustion CO₂ capture.³¹

3 Experimental

3.1 Yeast display of enzymes

The cDNA for bCA2 and hCA2 were cloned into the yeast surface display plasmid pCT-CON2 using standard molecular biology techniques. All cloning steps were performed in *E. coli*. Bovine CA2 cDNA in the pCMV-SPORT6 plasmid was ordered from Open Biosystems (clone ID: 7985245; Accession number: BC103260). Human CA2 cDNA in the pDONR221 plasmid was ordered from the Dana Farber/Harvard Cancer Center DNA Resource Core (plasmid ID: HsCD00005312; Refseq ID: NM 000067). The pCTCON2

plasmid was a generous gift from the Wittrup lab at MIT. Both CA2 genes contained internal BamHI restriction sites, which were removed using a Stratagene Quikchange Lightning Site Directed Mutagenesis Kit to make them compatible with the yeast display vector, pCTCON2. The genes were PCR amplified off of the plasmids and an upstream NheI restriction site and a downstream BamHI restriction site were added to make them compatible with the pCTCON2 plasmid. The yeast display vector pCTCON2 and the bCA2 and hCA2 PCR products were digested with the appropriate restriction enzymes and the digestion products were ligated into the vector. The CAH gene (from *S. thermophilus* LMG 18311 (Accession number: YP 140076) was codon optimized for *S. cerevisiae*, then synthesized and cloned into the pCTCON2 plasmid by DNA 2.0 (Menlo Park, CA). Deletion of the first 35 amino acids of the CAH protein was accomplished through site-directed mutagenesis using the protocol described previously.³⁸ Correct insertion of the genes of interest into the yeast-display plasmid was confirmed by DNA sequencing reactions prior to transformation of the plasmids into competent EBY100 cells. Transformed cells were propagated in SD-CAA media. Expression of the hCA2, bCA2, and CAH enzymes was induced by transferring the cells to fresh SG-CAA media at a concentration of 0.5 OD₆₀₀ and growing them for at least 24 hours at 22 °C.

3.2 Yeast display of mineralization peptides

Mineralization peptides were codon optimized for *S. cerevisiae* and were designed with the appropriate restriction enzyme sites for cloning into the pCTCON2 plasmid using the Gene Designer program from DNA 2.0. Oligonucleotides were synthesized using solid phase synthesis by IDT (Coralville, Iowa). The oligonucleotides were annealed, phosphorylated and inserted into the pCTON2 plasmid. Correct insertion of the genes of interest into the yeast-display plasmid was confirmed by DNA sequencing reactions prior to transformation of the plasmids into competent EBY100 *S. cerevisiae* cells. Transformed cells were propagated in SD-CAA media. Expression of the peptides was induced by transferring the cells to fresh SG-CAA media at a concentration of 0.5 OD₆₀₀ and growing them for at least 24 hours at 22 °C.

3.3 Measuring yeast display expression levels

Expression levels were measured as described previously.³⁹ After expression, 0.2 OD₆₀₀ cells were washed three times with 700 mL cold 1 PBS, 5 mg mL⁻¹ bovine serum albumin, sterile filtered (PBS-BSA). Washing consisted of spinning the cells, removing supernatant, and resuspending in wash solution. The cells were then resuspended in 100 mL of a 1 to 200 dilution of AlexaFluor 488 conjugated antibody (mouse anti-c-Myc 9B11 or mouse anti- HA 16B12) diluted in PBS-BSA. The cells were incubated for 30 to 60 minutes on ice. The cells were washed twice with PBS-BSA and were resuspended in 750 µL PBS-BSA. Cells were analyzed on a BD FACScan flow cytometer.

A Quantum Simply Cellular anti-Mouse IgG kit was used to quantitate the levels of expressed c-Myc or HA epitopes on the yeast cells according to the directions in the kit. Briefly, four populations of beads, each with a different level of antigen binding on it were stained with the same AlexaFluor 488 conjugated mouse antibody that was used to label the yeast cells. A fifth, unstained population of beads was added after staining and the beads

were analyzed on a BD FACScan flow cytometer using the same settings and on the same day as the yeast cells. A calibration curve was established by plotting the antibody binding capacity versus the peak channel for each population of stained beads. The Bang's Lab calibration file was used to provide a calibration curve.

The auxotrophic marker that is used to maintain selective pressure on the cells to retain the pCTCON2 yeast-display plasmid is not 100% effective. Thus, in any population of EBY100 cells that have been transformed with the pCTCON2 plasmid, some fraction of the cells do not express and display the protein of interest. Moreover, within the positive population of cells, there is a range of expression levels. This, in turn, affects the total numbers of proteins for the entire population of cells. To account for this, the flow cytometry data was processed by first calculating the percentage of cells that was expressing the full-length protein or peptide. The geometric mean of the positive population of cells was used to determine the average expression level per cell using the calibration curve from the Bang's lab beads. The "number of proteins per population of cells" was then calculated by multiplying the "percent expressing" by the "average expression level." If a positive population had a high and a low expression population, they were treated as separate populations and the sum of these was the number of proteins or peptides per population of cells.

3.4 Carbonic anhydrase activity assay

To test the activity of carbonic anhydrase isoforms, a modified version of the Wilbur–Anderson method was used.⁴⁰ First, the cells expressing the carbonic anhydrase were washed three times. Washing the cells was accomplished using a low speed centrifuge to pellet the cells, decanting the supernatant, then resuspending fully in cold distilled water. The cells were then resuspended in fifteen mL of the chilled assay buffer. Carbon dioxide gas was bubbled through a flask of stirred distilled water that was packed in ice for at least one hour to reach CO₂ saturation in the liquid (roughly 67 mM CO₂ at 3 °C). The reaction buffer, Tris–HCl, pH 8.8 (0.02 M) was chilled on ice for at least 1 hour. A pH electrode was 3-point calibrated at 3 °C. For the blank, fifteen mL of the Tris–HCl was added to a clean glass beaker with a small stir bar sitting in an ice bath. For the soluble carbonic anhydrase experiments, 200 µL of 0.1 mg mL⁻¹ enzyme was added to the buffer (Worthington Biochemical Corporation: LS001260). For the carbonic anhydrase displaying yeast cells, fifteen mL of the cells in assay buffer was added to the clean glass beaker with a small stir bar sitting in an ice bath. The pH electrode was added and allowed to reach equilibrium. Using the RS232 port, the data was collected and saved onto an attached computer. Once equilibrium was reached, 10 mL of the CO₂ saturated water was added. The pH was recorded every 1.5 seconds by the pH meter and saved to the computer. The raw pH values were converted to delta pH values (max pH – pH at time = *t*). The delta pH values were converted to percent reaction complete values (*e.g.*, 0% for *t* = 0 to 100% when the pH reached equilibrium).

3.5 Calculating activity of carbonic anhydrase

Using the data collected from the carbonic anhydrase activity assay, carbonic anhydrase activity was calculated using a modified version of Wilbur–Anderson units.⁴⁰ The units of

activity per nM of enzyme were calculated and the results were normalized to the blank reaction's results using the following equation:

$$\frac{(T_{blank\ average} - T_{sample\ average})}{T_{sample\ average}}$$

where $T_{blank\ average}$ is the average of the time that it took the blank reactions to reach 50% completion and the $T_{sample\ average}$ is the average time it took the sample reaction to reach 50% completion. Fifty percent completion was chosen because this was the point at which some of the reactions reached an inflection point. This inflection point was due to the weaker buffering capacity of tris buffer below pH 7.5.

3.6 Carbonic anhydrase stability studies

For the temperature stability studies, carbonic anhydrase displaying yeast or soluble carbonic anhydrase was washed three times as described above and resuspended in assay buffer either at the concentration to be used in the final assay (in the case of yeast displayed enzyme) or to a concentration of 0.1 mg mL⁻¹ (for the soluble carbonic anhydrase). The samples were then stored at 4 °C or in a 50 °C oven in sealed containers (to avoid evaporation of the buffer). For the pH stability studies, the samples were resuspended in buffers of the appropriate pH and were stored at 4 °C in sealed containers. Prior to use in the assay, the samples were then washed three times as described above. The cells were then resuspended in chilled assay buffer. The buffers used for the pH studies were: 65 mM phosphate–citrate buffer, pH 3.0; 72 mM phosphate–citrate buffer, pH 5.0; distilled water, pH 6.0; 81 mM phosphate–citrate buffer, pH 7.0.

3.7 Mineralization rate measurement

The mineralization rate of calcium carbonate was measured using calcium sensitive electrodes. The probes were calibrated using three standard solutions of 0.01 M, 0.05 M, and 0.1 M calcium chloride. Then 7.5 mL of 0.2 M CaCl₂ was placed in a 50 mL falcon tube with a magnetic stir bar and the tube was placed on a magnetic stir plate. Three hundred mL of calcium ionic strength adjuster (Orion 932011) was added to the solution and the stirring was set to 850 RPM. The yeast cells were prepped by washing several times with distilled water and then either 180 OD₆₀₀ or 18 OD₆₀₀ of cells were resuspended to a final volume of 7.7 mL (for the 2 × 10⁸ or the 2 × 10⁷ cells per mL samples, respectively). The calcium ion electrode was added to the sample and allowed to equilibrate. Then 2.5 mL of 0.1 M NaHCO₃ was added using a syringe pump set to inject at 5 mL min⁻¹ and the change in calcium ion concentration was measured. Using the RS232 port, the data was collected and saved onto an attached computer. The slope of the change in calcium ion concentration was calculated and converted to a value with units of moles L⁻¹ s⁻¹. Each peptide and concentration was measured in duplicate and values reported are averages of these measurements. The sample was then saved and analyzed by light microscopy and by X-ray diffraction to confirm the presence of calcium carbonate.

3.8 Polarized light microscopy and X-ray diffraction analysis

Samples for microscopy were prepared by pipetting a small aliquot directly out of the mineralization reaction onto a glass slide and covering with a glass coverslip. Cross-polarized microscopy was performed using orthogonal polarizing filters before and after the sample. XRD samples were prepared by taking roughly 50 mL out of a reaction, centrifuging for 10 minutes to pellet the sample, and removing the supernatant by decanting. If necessary, the sample was resuspended in a small amount of distilled water. The sample was transferred into an X-ray diffraction (XRD) sample holder. The sample was placed at 80 °C to dry and was analyzed on a Rigaku Powder Diffractometer using a 10 minutes scan. Crystal structure was verified by comparing to appropriate standard reference cards.

3.9 Lab-scale CO₂ mineralization reactor

A lab-scale CO₂ mineralization reactor was designed and built. This reactor was composed of a 0.25 L glass laboratory bottle with a threaded cap with a 65 mm diameter and a height of roughly 90 mm from the internal base to the neck. A custom-made stainless steel cap for the bottle was made that fit the threading on the bottle and that had three ports in the top. Two of the ports accommodated stainless steel tubing that could slide into and out of the port (to adjust the delivery height of the mock flue gas and the capture height of the off gas). Each port had a compression-tightened o-ring to ensure an airtight seal when the stainless steel tubing was in place. The third port accommodated the Ca²⁺-sensitive electrode. This electrode could slide in and out of the port to adjust the detection height. The port had a compression-tightened o-ring to ensure an airtight seal once the electrode was in place. The metal to glass connection between the cap and the bottle was not airtight, so petroleum jelly was applied to the threads every time the cap was put in place. All stainless steel connections were made using Teflon tape to ensure a tight seal. All stainless steel tubing that was used had a 1 mm inner diameter and the lengths of the connections were minimized in order to reduce the volumes inside of the tubing (50 cm from mass flow controller to gas injection site in reactor and 40 cm from reactor to CO₂ detector). All experiments were performed at atmospheric pressure. The result of this set-up was that all of the flue gas that was delivered to the reactor was collected by the off-gas port and was analyzed by the in-line CO₂ detector.

The temperature of the reactor was controlled using a temperature-controlled stir plate, wherein the thermocouple was placed into a solution of water surrounding the CO₂ reactor. The temperature of the liquid inside the reactor was thus controllable from 25 °C to 60 °C ± 2 °C and was verified to stay at the set temperature for at least 20 hours.

The mock flue gas was a custom-made mixture of 15% CO₂ and 85% N₂. The flow rate of the gas was controlled by an Alicat Scientific mass flow controller that was calibrated for that gas mixture. The % CO₂ in the off-gas was measured using an Alpha Omega Instruments 9510 analyzer with a built-in temperature controller to keep the temperature in the detector higher than the temperature in the reactor (so that condensation of water vapor would not occur in the detector).

For each reaction, the reactor was filled with the appropriate Ca^{2+} source, OH^- source, and yeast strain, the cap was placed on the bottle, and the system was purged with 100% N_2 . The signals from both the Ca^{2+} -sensitive electrode and the CO_2 detector were recorded using an attached computer. At time, $t = 0$, a solenoid valve was used to switch the gas source from the N_2 to the 15% CO_2 .

For the results reported in ESI Table 1,[†] the 0.25 L reactor was filled with 0.2 L of 0.1 M Tris base, 0.1 M CaCl_2 , and 67 nM bCA2 or bCA2-yeast (at a bCA2 concentration of 67 nM). The liquid was vigorously stirred using a magnetic stir bar set to roughly 700 RPM. The mock flue gas was injected directly into the bottom of the liquid with a flow rate of 0.1 liter per minute using stainless steel tubing with a 1 mm inner diameter, which resulted in small bubbles to maximize the absorption of the CO_2 into the liquid. The reaction was performed at 25 °C and at atmospheric pressure and was allowed to proceed to steady state (no change in CO_2 concentration in off-gas and no change in Ca^{2+} concentration in reactor). See ESI Fig. 4[†] for an image of the CO_2 capture reactor.

3.10 Process modeling

Microsoft Excel was used to calculate the mass balances at each process stage for the various species involved in the CO_2 capture process, including nitrogen, oxygen, carbon dioxide, the components of fly ash (or paper mill ash) water, calcium oxide, yeast, glucose, and the mineralized carbonate product. (Table 4, ESI Tables 6 and 8[†]). These mass balances were used to determine the minimum process equipment sizes.

Aspen Process Economic Analyzer V7.2.1 was used to determine the capital equipment costs. For special items not listed in Aspen Process Economic Analyzer, quotes were requested from suitable vendors. The purchase costs of the necessary equipment for the bCA2-yeast base case and the two alternate CaO cases are listed in Table 3, ESI Tables 5 and 7.[†] Additional infrastructure and set-up costs (including piping, steel, instrumentation, electrical, insulation, paint, and installation labor) were added to determine the direct costs associated with this process. Indirect costs, such as general and overhead costs, engineering costs, contract fees and contingencies were included in the final cost. See ESI Table 2[†] for detailed inside battery limit costs for the bCA2-yeast and fly ash base case. Finally, an additional 20% of the total direct and indirect costs was added for the integration of this process into an existing power plants infrastructure.

The operating costs were calculated based on the amount of electrical energy, cooling water, well cooling water, air, copper sulphate, and glucose necessary to operate the process. The operating costs are reported in ESI Table 3.[†] It was estimated that four additional workers would be needed to operate the system, that annual maintenance would be 3% of the capital costs, and that an additional 25% of labor and maintenance costs would be required for indirect costs. The capital equipment costs for a plant depreciation of 15 years and a conservative estimate of return on capital employed of 9% were calculated.

The cost of the full process was determined, including capital equipment, operating costs, labor, maintenance, plant depreciation, and return on capital employed. The annual cost of the process was divided by the annual CO_2 capture capacity or the annual solids production

(which includes CaCO₃, yeast and inactive materials in the CaO source). Table 5 shows these calculations for all processes.

3.11 Levelized cost of electricity calculation

The levelized cost of electricity calculation is described in detail in ESI Table 10[†] and the associated text. Briefly, levelized cost of electricity for a mineralized CO₂ product from our process was calculated by multiplying a widely accepted value for the cost of electricity without CO₂ capture at a pulverized coal power plant by the gross electricity production.³¹ This was added to the product of the cost of CO₂ capture for the process and the amount of CO₂ captured and the entire value was divided by the net electricity production. Finally, from this value was subtracted the product sale proceeds (price multiplied by production rate) divided by gross electricity production.

3.12 Heavy metal analysis

CO₂ was mineralized by dissolving coal fly ash (gift from Boston Sand and Gravel) or paper mill ash (gift from New England Organics) in stirred water. CO₂ was bubbled through the sample for several hours, or until mineralization was complete, as measured by a stabilization of the pH of the sample. Once the mineralization was complete, the water was removed using a filter unit with a 0.20 μm pore size. The sample was then sent to Galbraith Laboratories (Knoxville, TN) for analysis of silicon dioxide (ICP), mercury (EPA-SW846), cadmium (ICP), chromium VI (SM 3500 Cr D), lead (ICP), and arsenic (ICP).

4 Conclusions

In this work, engineered *S. cerevisiae* was used to enhance the hydration of CO₂, the mineralization rate of CaCO₃, and the settling time of the mineralized CaCO₃. Using the enhanced rates measured in a laboratory setting, an industrial scale model of the process was created. This model predicts a process using bCA2-yeast and fly ash is ~10% more cost effective per ton of CO₂ captured than a process with no biological molecules, a savings not realized by wild-type yeast and high-temperature stable recombinant CA2 alone or in combination.

The LCOE for the bCA2-yeast and fly ash process was calculated and was benchmarked against MEA absorption, which is a widely accepted baseline case for post combustion CO₂ capture. When comparing the bCA2-yeast and fly ash process to the MEA absorption process, it is important to recognize that the costs reported in Table 5 and Fig. 4 for the former include CO₂ capture and storage, whereas for the latter the costs only include CO₂ capture. Assuming that a downstream user for the mineralized CO₂ could be found, both a landfill tipping fee credit and a product sale price will lower the LCOE of the bCA2- yeast process. A range of values for both of these, based on literature reports and market research, was explored. While the bCA2-yeast and fly ash process LCOE is roughly three times higher than that for MEA absorption without the product being sold (*i.e.* \$0 tonne⁻¹ landfill tipping fee credit and \$0 tonne⁻¹ product sale price), if a mid-range tipping fee credit of \$20 ton⁻¹ and a sale price of \$20 ton⁻¹ are assumed, then the cost of this process is essentially the same as MEA absorption (see Fig. 4).

Supplementary Material

Refer to Web version on PubMed Central for supplementary material.

Acknowledgments

This work was supported by Eni, S.p.A (Italy) through the MIT Energy Initiative Program. R.B. is grateful for funding from the NIH Biotechnology Training Program and from the Siebel Foundation. R.B. would like to acknowledge Dane Witttrup, Ed DeLong, and Elizabeth Wood for helpful conversations throughout the project. The authors would like to acknowledge the MIT Center for Materials Science and Engineering and Dr Scott Speakman for help with XRD analysis, the MIT Biopolymers & Proteomics Core Facility for DNA sequencing services, and the MIT Central Machine Shop for help with the CO₂ capture reactor.

Notes and references

1. Lackner KS. *Science*. 2003; 300:1677–1678. [PubMed: 12805529]
2. Durwood Zaelke, OY.; Andersen, S. *Scientific Synthesis of Calera Carbon Sequestration and Carbonaceous By-Product Applications*, Donald Bren School of Environmental Science and Management. University of California; Santa Barbara: 2011.
3. House KZ, House CH, Schrage DP, Aziz MJ. *Environ Sci Technol*. 2007; 41:8464–8470. [PubMed: 18200880]
4. House KZ, Schrag DP, Harvey CF, Lackner KS. *Proc Natl Acad Sci USA*. 2006; 103:12291–12295. [PubMed: 16894174]
5. Belcher AM, Wu XH, Christensen RJ, Hansma PK, Stucky GD, Morse DE. *Nature*. 1996; 381:56–58.
6. Falini G, Albeck S, Weiner S, Addadi L. *Science*. 1996; 271:67–69.
7. Helman Y, Natale F, Sherrell RM, LaVigne M, Starovoytov V, Gorbunov MY, Falkowski PG. *Proc Natl Acad Sci USA*. 2008; 105:54–58. [PubMed: 18162537]
8. Miyamoto H, Miyashita T, Okushima M, Nakano S, Morita T, Matsushiro A. *Proc Natl Acad Sci U S A*. 1996; 93:9657–9660. [PubMed: 8790386]
9. Tong H, Wan P, Ma WT, Zhong GR, Cao LX, Hu JM. *J Struct Biol*. 2008; 163:1–9. [PubMed: 18485735]
10. Lee BD, Apel WA, Walton MR. *Biotechnol Prog*. 2004; 20:1345–1351. [PubMed: 15458316]
11. Phelps, TJ.; Lauf, RJ.; Roh, Y. *Biom mineralization for Carbon Sequestration*. Oak Ridge National Laboratory; 2003.
12. Roh, Y.; Phelps, TJ.; McMillan, AD.; Lauf, RJ. *Utilization of biomineralization processes with fly ash for carbon sequestration*. National Energy Technology Laboratory; 2000.
13. Bond GM, Stringer J, Brandvold DK, Simsek FA, Medina MG, Egeland G. *Energy Fuels*. 2001; 15:309–316.
14. Cowan RM, Ge JJ, Qin YJ, McGregor ML, Trachtenberg MC. *Adv Membr Technol Appl*. 2003; 984:453–469.
15. Liu N, Bond GM, Abel A, McPherson BJ, Stringer J. *Fuel Process Technol*. 2005; 86:1615–1625.
16. Fan LH, Liu N, Yu MR, Yang ST, Chen HL. *Biotechnol Bioeng*. 2011; 108:2853–2864. [PubMed: 21732326]
17. Borchert, M.; Saunders, P. US Pat. US 7,892,814 B2. 2011.
18. Daigle, R.; Desrochers, M. US Pat. US 7,521,217 B2. 2009.
19. Boder ET, Witttrup KD. *Nat Biotechnol*. 1997; 15:553–557. [PubMed: 9181578]
20. Boder ET, Witttrup KD. *Applications of Chimeric Genes and Hybrid Proteins, Pt C*. 2000; 328:430–444.
21. Kernohan JC. *Biochim Biophys Acta*. 1965; 96:304–317. [PubMed: 14298834]
22. Elhadj S, De Yoreo JJ, Hoyer JR, Dove PM. *Proc Natl Acad Sci USA*. 2006; 103:19237–19242. [PubMed: 17158220]
23. Fakhruddin RF, Minullina RT. *Langmuir*. 2009; 25:6617–6621. [PubMed: 19505153]

24. Kiil S, Michelsen ML, Dam-Johansen K. *Ind Eng Chem Res.* 1998; 37:2792–2806.
25. Lundy, S. *Wet Flue Gas Desulfurization Technology Evaluation– Project Number 11311-000.* Chicago, IL: 2003.
26. Riesenfeld, FC.; Kohl, AL. *Gas purification.* 2. Gulf Pub. Co; Houston: 1974.
27. Stolaroff JK, Keith DW, Lowry GV. *Environ Sci Technol.* 2008; 42:2728–2735. [PubMed: 18497115]
28. Bhattacharya S, Nayak A, Schiavone M, Bhattacharya SK. *Biotechnol Bioeng.* 2004; 86:37–46. [PubMed: 15007839]
29. Finkenrath, M. *Cost and Performance of Carbon Dioxide Capture from Power Generation.* International Energy Agency; 2011.
30. Rubin, R.; Rao, AB.; Chen, C. *Proc. of 28th International Technical Conf. on Coal Utilization & Fuel Systems;* Clearwater, FL. 2003.
31. Woods, MC.; Capicotto, P.; Haslbeck, J.; Kuehn, N.; Matuszewski, M.; Pinkerton, LL.; Rutkowski, MD.; Schoff, RL.; Vaysman, V. *Cost and Performance Baseline for Fossil Energy Plants Volume 1: Bituminous Coal and Natural Gas to Electricity Final Report.* N.E.T. Laboratory; 2010. p. 1
32. Klein-Marcuschamer D, Oleskowicz-Popiel P, Simmons BA, Blanch HW. *Biotechnol Bioeng.* 2012; 109:1083– 1087. [PubMed: 22095526]
33. van Beilen JB, Li Z. *Curr Opin Biotechnol.* 2002; 13:338–344. [PubMed: 12323356]
34. Zhuang J, Marchant MA, Nokes SE, Strobel HJ. *Appl Eng Agr.* 2007; 23:679–687.
35. van Haaren R, Themelis N, Goldstein N. *Biocycle.* 2010:16–23.
36. http://www.concreteconstruction.net/images/FlyAsh_tcm45-346438.pdf.
37. <http://www.icis.com/chemicals/channel-info-chemicals-a-z/>.
38. Makarova O, Kamberov E, Margolis B. *BioTechniques.* 2000; 29:970–972. [PubMed: 11084856]
39. Chao G, Lau WL, Hackel BJ, Sazinsky SL, Lippow SM, Wittrup KD. *Nat Protoc.* 2006; 1:755–768. [PubMed: 17406305]
40. Wilbur KM, Anderson NG. *J Biol Chem.* 1948; 176:147–154. [PubMed: 18886152]

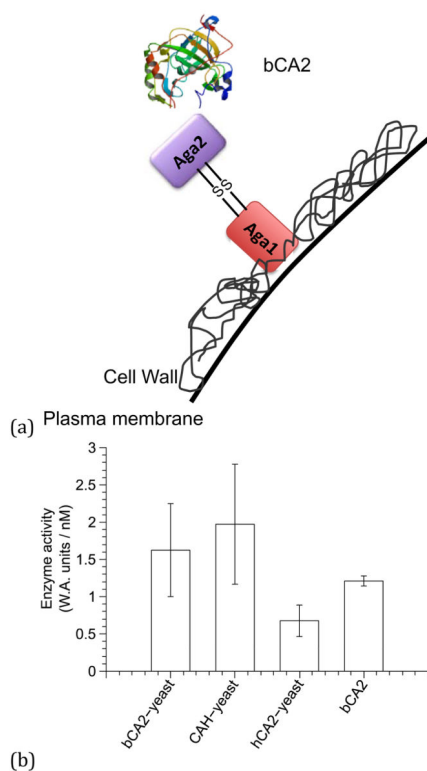
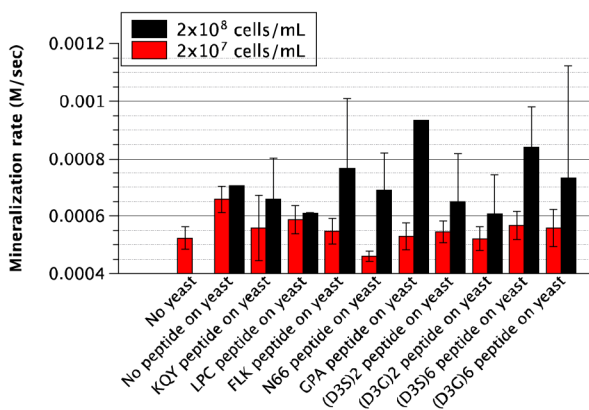
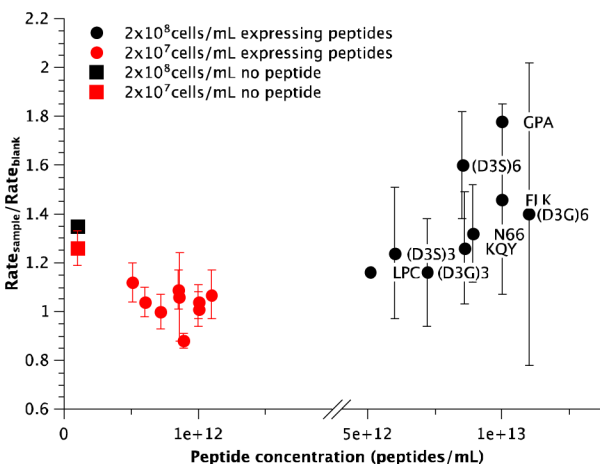


Figure 1.

A) In the yeast display system used in this work, an *aga2-bCA2* gene fusion results in an Aga2-bCA2 protein fusion that is linked via disulfide bonds to Aga1 on the surface of the yeast cells. Aga1 is covalently attached to the b-glucan in the extracellular matrix of the yeast cell wall. More than 10^5 fusion proteins can be displayed on each yeast cell. Image of bCA2 from the RCSB PDB (www.pdb.org) of PDB ID 1V9E (R. Saito, T. Sato, A. Ikai and N. Tanaka, *Acta Crystallographica Section D-Biological Crystallography*, 2004, **60**, 792–795.) B) The yeast display system was used to display three isoforms of carbonic anhydrase on the surface of the yeast cells. Each isoform demonstrated CO_2 hydration activity that was comparable to that of soluble, recombinantly produced bCA2.



(a)



(b)

Figure 2.

Measurement of mineralization rate enhancement by yeast-displayed peptides (a) The mineralization rate of CaCO_3 in the mineralization reactor was measured for each of the nine strains of peptide-expressing yeast, as well as for a no peptide strain of yeast, at two concentrations of cells: 2×10^8 cells mL^{-1} and 2×10^7 cells mL^{-1} . The baseline mineralization rate was measured without yeast. Each sample was measured in duplicate and the averages are reported. Error bars represent one standard deviation. (b) The mineralization rates for each sample were normalized to the rate of the blank (no yeast) sample and are plotted against the concentration of peptide in the sample. The yeast with no peptide is plotted at an arbitrary concentration of 1×10^{11} peptides mL^{-1} so that it can be viewed on the same chart as the peptide-yeast strains.

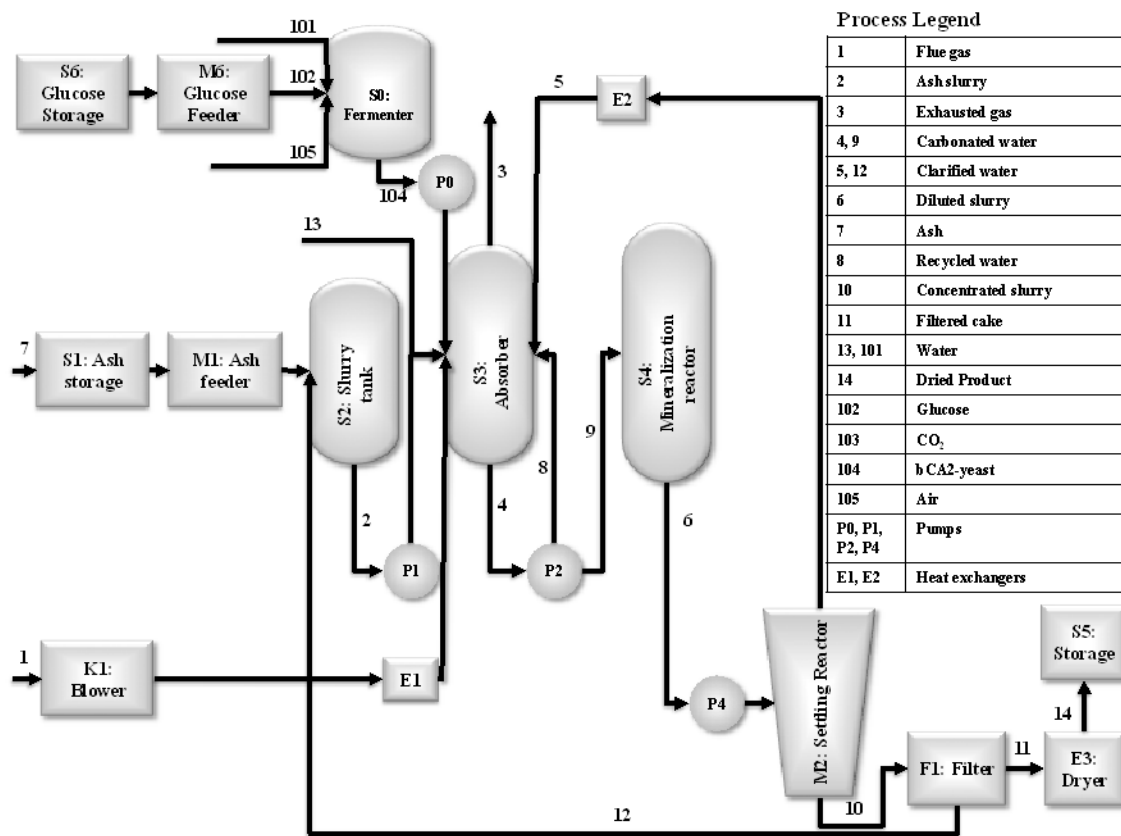


Figure 3. Process diagram for CO₂ mineralization processes using bCA2-yeast and fly ash or bCA2-yeast and paper mill ash. Equipment sizes and costs for the fly ash and bCA2-yeast process are listed in table 4. Mass balances for the fly ash and bCA2-yeast process are listed in supplementary table 3. Equipment sizes and costs for the paper mill ash and bCA2-yeast process are listed in supplementary table 5. Mass balances for the paper mill ash and bCA2-yeast process are listed in supplementary table 6.

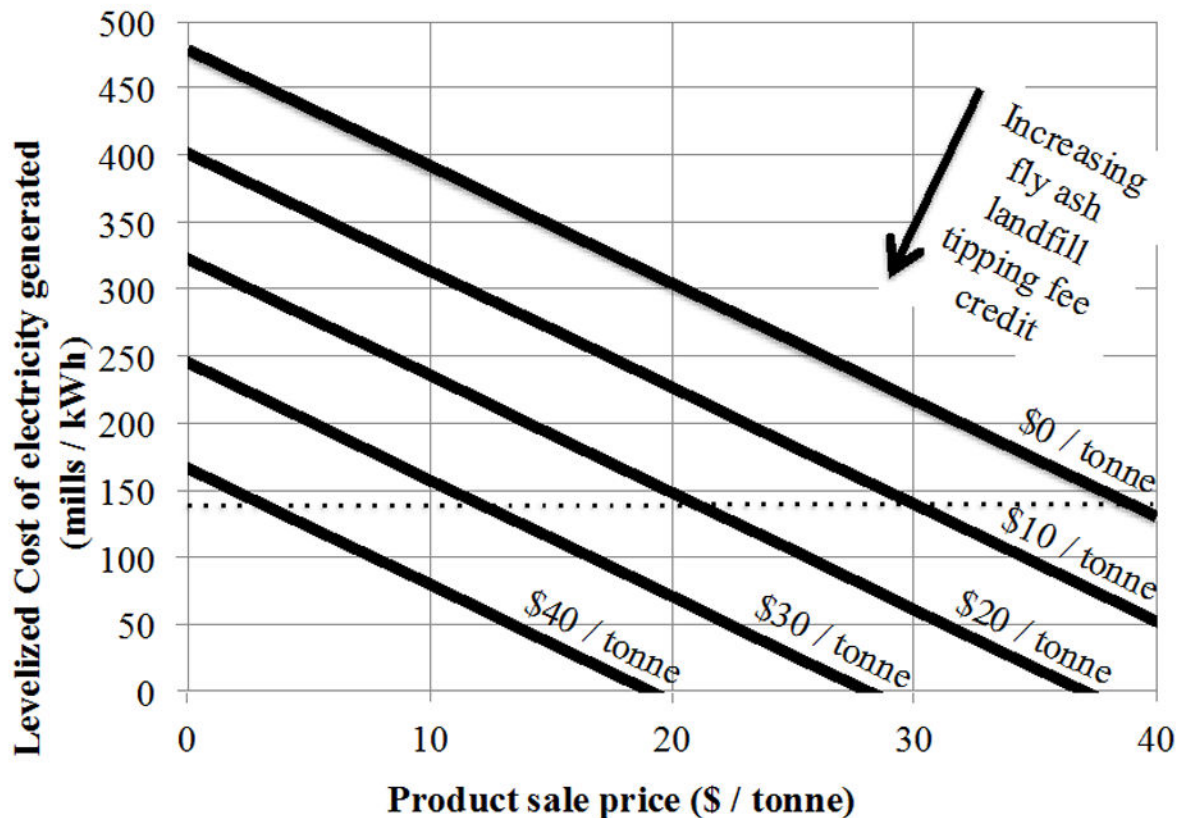


Figure 4.

This figure shows the impact that the fly ash landfill tipping fee credit and the sale price of the mineralized CO₂ product have on the levelized cost of electricity (LCOE) for a pulverized coal subcritical power plant with a CO₂ mineralization process utilizing fly ash and bCA2-yeast. Each of the thick black lines shows the LCOE for a set fly ash landfill tipping fee. The x-axis is the product sale price and the y-axis is the LCOE of the process. The horizontal dashed line at 139 mills/kWh represents the reported LCOE for a pulverized coal subcritical power plant capturing 90% of the CO₂ using an MEA absorption process reported by Woods, et al. 2010. Note that the LCOE for the MEA process does not include CO₂ storage costs. The calculations underlying this figure are described in supplementary table 10

Table 1

These nine peptides were displayed on the surface of the yeast cells using the yeast display system described in figure 1. The yeast-displayed peptides were evaluated for their ability to enhance the mineralization rate of CaCO_3 .

Mineralization peptide	Source	Size (amino acids)	Sequence	Expression level used for testing (peptides per 2×10^7 cells)
GPA	From glycoporphin A, the calcium binding protein in <i>Emiliana huxley</i>	12	PEVPEGAFDTAI	1×10^{12}
N66	From the region of the protein nacrein though to be responsible for CaCO_3 mineralization	12	(GNN) ₄	8.9×10^{11}
LPC	Control peptide with no negative charges	12	(LPC) ₄	5.1×10^{11}
KQY	Control peptide with positive charges	12	(KQY) ₄	8.6×10^{11}
FLK	Control peptide with positive charges	12	(FLK) ₄	1×10^{12}
(D ₃ G) ₆	Synthetic peptide with demonstrated CaCO_3 mineralization enhancement properties	27	(D ₃ G) ₆ D ₃	1.1×10^{12}
(D ₃ G) ₃	Shortened version of above	12	(D ₃ G) ₃ D ₃	7.2×10^{11}
(D ₃ S) ₆	Synthetic peptide with demonstrated CaCO_3 mineralization enhancement properties	27	(D ₃ S) ₆ D ₃	8.5×10^{11}
(D ₃ S) ₃	Shortened version of above	12	(D ₃ S) ₃ D ₃	6.0×10^{11}

Table 2

Reactions in the CO₂ mineralization process are listed with the biological catalysts for each reaction and the uncatalyzed and catalyzed reaction rates measured in the lab. The single arrow in reactions indicates that the reactions are treated as irreversible under the conditions proposed for this work.

	Reaction	Catalyzed by	Uncatalyzed rate parameter	Enhanced rate parameter
1	$\text{CO}_{2(aq)} + \text{H}_2\text{O} \rightarrow \text{HCO}_3^- + \text{H}^+$	bCA2-yeast	$0.045 \frac{1}{\text{second}}$	$6 \times 10^5 \frac{1}{\text{second}} [a]$
	Reaction	Catalyzed by	Uncatalyzed mineralization rate	Enhanced mineralization rate
2	$\text{H}^+ + \text{HCO}_3^- + \text{Ca}^{2+} + 2\text{OH}^- \rightarrow \text{CaCO}_3 + \text{H}_2\text{O}$	GPA-yeast	$5.2 \times 10^{-4} \frac{\text{moles CaCO}_3}{(\text{L})(\text{second})} [b]$	$9.3 \times 10^{-4} \frac{\text{moles CaCO}_3}{(\text{L})(\text{second})} [b]$
		No peptide yeast	$5.2 \times 10^{-4} \frac{\text{moles CaCO}_3}{(\text{L})(\text{second})} [b]$	$6.3 \times 10^{-4} \frac{\text{moles CaCO}_3}{(\text{L})(\text{second})} [b]$

[a] Conservative estimate based on activity level comparisons to soluble bCA2.

[b] From figure 2.

Table 3

Equipment sizes and costs for CO₂ mineralization process using fly ash and bCA2-yeast. Equipment costs were determined using Aspen Process Economic Analyzer V7.2.1, where applicable. For equipment not available in Aspen Process Economic Analyzer, estimated costs were provided from equipment vendors. Costs are in US dollars for a US location in 2011. The sum of the direct equipment costs, the man power for this equipment, and the indirect costs associated with this equipment is the total inside battery limits investment for this process. See supplementary table 2 for details.

Item ID	Equipment	Size	Purchase cost (thousand \$)	Direct cost (thousand \$)
S0	Fermenter	3.83 m ³	48	157
S1	Ash storage	884 m ³	188	275
S2	Slurry tank	28.3 m ³	89	203
S3	Absorber	11.3 m ³	31	164
S4	Mineralization reactor	17.7 m ³	58	161
S5	Product storage	180 m ³	0	166
S6	Glucose storage	5 m ³	36	224
M1	Ash feeder (conveyer belt)	81.7 tonne/hr	45	128
M2	Settling reactor	577 m ³	86	276
M6	Glucose feeder (rotary feeder)	25 kg/hr	4	7
P0	Yeast pump	0.1 L/sec	6	25
P1	Circulation pump	7 L/sec	7	39
P2	Recirculation pump	40 L/sec	23	110
P4	Diluted slurry pump	20 L/sec	9	44
E1	Flue gas cooler (heat exchanger)	3.54×10 ⁴ kcal/hr	14	72
E2	Clarified water cooler (heat exchanger)	2.39×10 ⁵ kcal/hr	13	69
E3	Plate dryer	4700 L/hr	1875	1875
F1	Filter press	25 m ³ /hr	852	852
K1	Flue gas blower	3000 m ³ /hr	5	15
	Unscheduled items			13
Total				4872

Table 4

Mass balance for CO₂ mineralization process using fly ash and bCA2-yeast. The streams in this table correspond to those with matching labels in figure 3.

	1 Flue gas		2 Ash slurry		3 Exhausted gas		4 Carbonated water		5 Clarified water	
	Rate [ton/h]	Comp. %wt	Rate [ton/h]	Comp. %wt	Rate [ton/h]	Comp. %wt	Rate [ton/h]	Comp. %wt	Rate [ton/h]	Comp. %wt
N ₂	2.8	70.2			2.8	85.0				
O ₂	0.15	3.7			0.15	4.5				
CO ₂	0.81	20.5			0.12	3.7				
H ₂ O	0.22	5.6	19.9	79.4	0.22	6.8	137.0	92.2	47.6	100.0
SiO ₂			2.6	10.3			5.1	3.5		
Al ₂ O ₃			1.3	5.1			2.6	1.7		
Fe ₂ O ₃			0.41	1.6			0.82	0.55		
CaO							3.1	2.1		
CaCO ₃										
Glucose										
bCA2-yeast							1.5E-02	1.0E-02		
tonne/hr	3.9	100.0	24.1	96.5	3.3	100.0	148.6	100.0	47.6	100.0

	6 Diluted slurry		7 Ash		8 Recycled water		9 Carbonated water		10 Concentrated slurry	
	Rate [ton/h]	Comp. %wt	Rate [ton/h]	Comp. %wt	Rate [ton/h]	Comp. %wt	Rate [ton/h]	Comp. %wt	Rate [ton/h]	Comp. %wt
N ₂										
O ₂										
CO ₂										
H ₂ O	68.5	92.2			68.5	92.2	68.5	92.2	20.9	78.2
SiO ₂	2.6	3.5	2.6	50.0	2.6	3.5	2.6	3.5	2.6	9.6
Al ₂ O ₃	1.3	1.7	1.3	25.0	1.3	1.7	1.3	1.7	1.3	4.8
Fe ₂ O ₃	0.41	0.55	0.41	8.0	0.41	0.55	0.41	0.55	0.41	1.5
CaO			0.87	17.0						

	6 Diluted slurry		7 Ash		8 Recycled water		9 Carbonated water		10 Concentrated slurry	
	Rate [ton/h]	Comp. %wt	Rate [ton/h]	Comp. %wt	Rate [ton/h]	Comp. %wt	Rate [ton/h]	Comp. %wt	Rate [ton/h]	Comp. %wt
CaCO ₃	1.6	2.1			1.6	2.1	1.6	2.1	1.6	5.8
Glucose										
bCA2-yeast									7.5E-03	0.028
tonne/hr	74.3	100.0	5.1	100.0	74.3	100.0	74.3	100.0	26.7	100.0

	11 Filtered cake		12 Clarified water		13 Water		14 Dried Product	
	Rate [ton/h]	Comp. %wt	Rate [ton/h]	Comp. %wt	Rate [ton/h]	Comp. %wt	Rate [ton/h]	Comp. %wt
N ₂								
O ₂								
CO ₂								
H ₂ O	1.0	15.0	19.9	100.0	1.03	100.0	0.029	0.50
SiO ₂	2.6	37.5					2.57	43.8
Al ₂ O ₃	1.3	18.7					1.28	21.9
Fe ₂ O ₃	0.41	6.0					0.41	7.0
CaO								
CaCO ₃	1.6	22.7					1.56	26.6
Glucose								
bCA2-yeast	7.5E-03	0.11					7.5E-03	1.3E-01
tonne/hr	6.9	100.0	19.9	100.0	1.0	100.0	5.9	100.0

	101 Water		102 Glucose		103 CO2		104 bCA2-yeast		105 Air	
	Rate [ton/h]	Comp. %wt	Rate [ton/h]	Comp. %wt	Rate [ton/h]	Comp. %wt	Rate [ton/h]	Comp. %wt	Rate [ton/h]	Comp. %wt
N ₂									21.4	76.7
O ₂	8.0E-03	11.3							6.5	23.3
CO ₂										
H ₂ O	0.063	88.7			0.011	100.0	0.068	90.0		
SiO ₂										

	101 Water		102 Glucose		103 CO2		104 bCA2-yeast		105 Air	
	Rate [ton/h]	Comp. %wt	Rate [ton/h]	Comp. %wt	Rate [ton/h]	Comp. %wt	Rate [ton/h]	Comp. %wt	Rate [ton/h]	Comp. %wt
Al ₂ O ₃										
Fe ₂ O ₃										
CaO										
CaCO ₃										
Glucose			0.015	100.0						
bCA2-yeast							7.5E-03	10.0		
tonne/hr	0.071	100.0	0.015	100.0	0.011	100.0	0.075	100.0	27.9	100.0

Table 5

Process costs for the various CO₂ mineralization process designs. An example of the ISBL investment cost calculation for the bCA2-yeast and fly ash process is shown in greater detail in supplementary table 2. An example of the operating cost calculation for the bCA2-yeast and fly ash process is shown in greater detail in supplementary table 3.

Process Number	1	2	3	4	5	6	7	8	9
Description	bCA2-yeast	Hypothetical 10x mineralization rate enhancement	No dryer in process*	No biological components	Wild-type yeast purchased at market price	Recombinantly produced high temp CA2	Wild-type yeast and recombinantly produced high temp CA2	Paper mill ash and bCA2-yeast****	Pre-carbonation leached CaO and bCA2-yeast
Units									
PROCESS DETAILS									
CaO source	Fly ash	Fly ash	Fly ash	Fly ash	Fly ash	Fly ash	Fly ash	Paper mill ash	CaO-leached fly ash
Process modifications	Base case	Removal of S4 and P4	Removal of E3	Larger S4, larger S3, larger M2	Outside source of wild-type yeast; Removal of S6, M6, S0, P0	Outside source of CA2; larger S3, larger M2; Removal of S6, M6, S0, P0, E2; smaller E1, Removal of well cooling water.	Outside source of CA2; outside source of wild-type yeast; Removal of S6, M6, S0, P0, E2; Smaller E1; Removal of well cooling water.	Use of paper mill ash as CaO source in lieu of coal fly ash	Use of CaO-leached fly ash in lieu of coal fly ash.
Capacity	5830	5830	5830	5830	5830	5830	5830	2388	1565
Calcium carbonate in dried product	27%	27%	22%	27%	27%	27%	27%	62%	100%
INVESTMENT COST									
Total Investment (ISBL)	\$7,536	\$7,256	\$4,971	\$8,287	\$7,144	\$7,709	\$7,079	\$4,703	\$6,989
<i>Total Direct Cost</i>	\$5,509	\$5,304	\$3,634	\$6,058	\$5,223	\$5,635	\$5,175	\$3,438	\$5,109
<i>Total Indirect Cost</i>	\$2,027	\$1,952	\$1,337	\$2,229	\$1,922	\$2,074	\$1,904	\$1,265	\$1,880
OSBL (20% of ISBL)	\$1,507	\$1,451	\$994	\$1,657	\$1,429	\$1,542	\$1,416	\$941	\$1,398
Total Investment Cost (ISBL + OSBL)	\$9,043	\$8,707	\$5,965	\$9,945	\$8,573	\$9,250	\$8,495	\$5,643	\$8,386
OPERATING COST									
Total Operating Cost	-\$0.0145179	-\$0.0145179	-\$0.0145179	-\$0.0148151	-\$0.0115986	-\$0.0147564	-\$0.0115400	-\$0.0090722	\$0.0080562
<i>Electric Energy</i>	\$0.0009428	\$0.0009428	\$0.0009428	\$0.0009452	\$0.0009452	\$0.0009428	\$0.0009428	\$0.0011370	\$0.0084661
<i>Cooling Water</i>	\$0.0000003	\$0.0000003	\$0.0000003	\$0.0000003	\$0.0000003	\$0.0000003	\$0.0000003	\$0.0000057	\$0.0000120
<i>Well cooling water</i>	\$0.0000041	\$0.0000041	\$0.0000041	\$0.0000041	\$0.0000041	\$0.0000000	\$0.0000000	\$0.0000101	\$0.0000154
<i>Air</i>	\$0.0000000	\$0.0000000	\$0.0000000	\$0.0000000	\$0.0000000	\$0.0000000	\$0.0000000	\$0.0000000	\$0.0000000
<i>Market purchased wild-type yeast</i>	\$0.0000000	\$0.0000000	\$0.0000000	\$0.0000000	\$0.0032164	\$0.0000000	\$0.0032164	\$0.0000000	\$0.0000000
<i>Copper sulfate</i>	\$0.0000091	\$0.0000091	\$0.0000091	\$0.0000000	\$0.0000000	\$0.0000000	\$0.0000000	\$0.0000223	\$0.0000340
<i>Glucose</i>	\$0.0002904	\$0.0002904	\$0.0002904	\$0.0000000	\$0.0000000	\$0.0000000	\$0.0000000	\$0.0003047	\$0.0009106
<i>Market purchased high temperature CA2</i>	\$0.0000000	\$0.0000000	\$0.0000000	\$0.0000000	\$0.0000000	\$0.0000652	\$0.0000652	\$0.0000000	\$0.0000000

Process Number	1	2	3	4	5	6	7	8	9	
Description	Units	bCA2-yeast	Hypothetical 10x mineralization rate enhancement	No dryer in process*	No biological components	Wild-type yeast purchased at market price	Recombinantly produced high temp CAZ	Wild-type yeast and recombinantly produced high temp CAZ	Paper mill ash and bCA2-yeast****	Pre-carbonation leached CaO and bCA2-yeast
<i>Landfill tipping fee credit for ash (\$17.89/tonne)**</i>	<i>\$/kg product</i>	-\$0.0157647	-\$0.0157647	-\$0.0157647	-\$0.0157647	-\$0.0157647	-\$0.0157647	-\$0.0157647	-\$0.0105521	-\$0.0013819
FIXED COST										
Total Fixed Cost	\$/kg product	\$0.0157	\$0.0154	\$0.0132	\$0.0164	\$0.0153	\$0.0158	\$0.0152	\$0.0316	\$0.0564
Total Direct Cost	\$/kg product	\$0.0125	\$0.0123	\$0.0106	\$0.0131	\$0.0122	\$0.0127	\$0.0122	\$0.0253	\$0.0451
Labor (4 @ \$54K/yr)***	\$/kg product	\$0.0046	\$0.0046	\$0.0046	\$0.0046	\$0.0046	\$0.0046	\$0.0046	\$0.0113	\$0.0173
Maintenance (3%/yr)***		\$0.00582	\$0.00560	\$0.00384	\$0.00640	\$0.00552	\$0.00595	\$0.00546	\$0.00886	\$0.02010
Direct overhead (45% labor cost)		\$0.00208	\$0.00208	\$0.00208	\$0.00208	\$0.00208	\$0.00208	\$0.00208	\$0.00509	\$0.00776
Total Indirect Cost (25% of direct cost)	\$/kg product	\$0.0031	\$0.0031	\$0.0026	\$0.0033	\$0.0031	\$0.0032	\$0.0030	\$0.0063	\$0.0113
PRODUCT COSTS										
Cash Cost (Operating Cost + Fixed Cost)	\$/kg product	\$0.0011	\$0.0009	-\$0.0013	\$0.0016	\$0.0037	\$0.0011	\$0.0037	\$0.0225	\$0.0645
Total Production Cost (Cash Cost + 15 yr Depreciation cost)	\$/kg product	\$0.0141	\$0.0133	\$0.0072	\$0.0158	\$0.0159	\$0.0143	\$0.0158	\$0.0422	\$0.1091
Depreciation (15 years)***	\$/kg product	\$0.0129	\$0.0124	\$0.0085	\$0.0142	\$0.0123	\$0.0132	\$0.0121	\$0.0197	\$0.0447
Total Cost (Production Cost + 9 yr ROCE)	\$/kg product	\$0.0315	\$0.0301	\$0.0187	\$0.0350	\$0.0325	\$0.0322	\$0.0322	\$0.0688	\$0.1694
ROCE***	\$/kg product	\$0.0175	\$0.0168	\$0.0115	\$0.0192	\$0.0165	\$0.0179	\$0.0164	\$0.0266	\$0.0603
Total Product Cost	\$/tonne product	\$31.5	\$30.1	\$18.7	\$35.0	\$32.5	\$32.2	\$32.2	\$68.8	\$169.4
CO₂ CAPTURE COSTS										
Total CO ₂ Capture Cost	\$/tonne CO ₂	\$268	\$256	\$159	\$297	\$276	\$273	\$274	\$239	\$386
Cost difference per tonne of carbon dioxide mineralized	(\$/tonne)		-\$12	-\$109	\$29	\$8	\$5	\$6	-\$28	\$118

* The removal of the dryer generates product that is only 85% dry which may be more challenging to sell. See supplementary table 9 for the cost associated with this modification if product cannot be sold and landfill tipping fee credit cannot be redeemed.

** This value for the landfill tipping fee comes from Woods, et al. 2010.

*** An 8000 hour year was used to convert labor and maintenance to an hourly cost and to calculate the depreciation and ROCE.

**** The paper mill ash process costs do not account for the transport of the paper mill ash to the CO₂ capture facility.